JOURNAL OF GEOPHYSICAL RESEARCH, VOL. 106, NO. D24, PAGES 33,529–33,541, DECEMBER 27, 2001

Near-surface climate in the boreal forest

Alan K. Betts and John H. Ball
Atmospheric Research, Pittsford, Vermont

J. Harry McCaughey
Department of Geography, Queen's University, Kingston, Ontario, Canada

Abstract. This paper addresses processes that affect near-surface climate over the boreal forest, using data from the Boreal Ecosystem-Atmosphere Study (BOREAS) northern study area just west of Thompson, Manitoba. The boreal forest is marked by a very large seasonal cycle with below-freezing temperatures for half the year. The freezing and thawing of the soil plays an important role in the climate at high latitudes. It moderates winter temperatures (together with the insulating snow cover), because during the freeze process, the effective heat capacity of the soil is greatly increased, and it introduces a significant lag into the climate system. Perhaps the most important consequence is that water is unavailable for evaporation and photosynthesis until snow melts and the ground thaws, which occurs late in spring. As a result, in April and in early May, relative humidity (RH) is a minimum, the surface sensible heat flux is large, and the daytime boundary layer (BL) is very deep, because of this unavailability of water. The situation reverses in the fall, when the ground is warmer than the cooling atmosphere, and mean RH is high and BL depths low. This asymmetry between spring and fall can be seen in both seasonal and diurnal cycles. The forest is heterogeneous, and there is a marked difference in summer in daytime evaporative fraction between the conifers and the deciduous forest and fens. However, above the forest the daytime BL has a strong homogenizing effect, and it is the dominant coniferous forest that controls the mean BL depth. The impact of recent rainfall, stored on the canopy, in the surface moss layer, and in the top soil layer can be readily seen in summer. BL depths rise on succeeding days without rain. A comparison of the fen and young jack pine sites shows the important role of the stomatal control by conifers on transpiration. Since evaporation goes down at high net radiation and low RH for conifer sites, it is clear that the low RH and high BL depth over the forest are a direct consequence of stomatal control. At night, however, temperature, relative humidity, and CO_2 are quite heterogeneous under the stable BL. We show that uncoupling of the stable BL at night inside the forest canopy occurs at low wind speeds and high outgoing net radiation and can lead to a 5K cooling within the canopy.

1. Introduction

The purpose of this paper is to summarize and interpret some of the measurements from the Boreal Ecosystem-Atmosphere Study (BOREAS), collected between March 1994 and October 1996 at several sites in the BOREAS northern study area (NSA) just west of Thompson, Manitoba. Our focus is on the surface thermodynamic variables and the surface energy balance, although we will also address briefly the diurnal and seasonal cycle of CO_2 and the net surface CO_2 flux. The partition of the net radiation at the surface into the sensible and latent heat fluxes plays a key role in influencing weather and climate over land, on both diurnal and seasonal timescales. In current global forecast and climate models, this land surface boundary condition is computed using many submodels (for the subsurface hydrology, vegetation, surface and boundary layers, radiation and clouds, for example). Despite improvements in many of these components in recent years, global forecast models still suffer from errors in their land surface parameterizations, especially over the boreal forest [e.g., *Betts et al.*, 1998]. These errors introduce systematic biases in the model climatology, which are one factor limiting medium-range and seasonal forecast skill and our ability to model the present day climate. This paper focuses on what was learned from the BOREAS observations about the land surface processes and climate. A companion paper discusses the improvements in the European Centre for Medium-Range Weather Forecasts (ECMWF) model at high latitudes, which resulted from reformulating the land surface model based in part on results from BOREAS [*Betts et al.*, this issue; *Van den Hurk et al.*, 2000].

From a climatic perspective, two key factors are important. The first is the surface radiation budget, which is determined by season, latitude, atmospheric aerosol, and cloud cover, as well as the surface albedo, near-surface temperature, and moisture. The high-latitude coniferous forests have a very low surface albedo in summer, around (0.08-0.09) for spruce and a little higher (0.09-0.13) for jack pine, and rather low values in winter, typically <0.2 [*Betts and Ball*, 1997; *Joiner et al.*, 1999a], since the canopy shades the snow from the low-elevation angle solar insolation. *Viterbo and Betts* [1999] discuss the large impact on the ECMWF model of correcting errors in the forest albedo in spring before snowmelt. The second factor is the partition of the net radiation minus ground heat flux into the sensible and latent heat fluxes to the atmosphere, which is controlled over land by the availability of water for evaporation

Paper number 2001JD900047.
0148-0227/01/2001JD900047$09.00

(which is dramatically affected by the seasonal cycle of soil freezing), and by the biophysical controls on transpiration in the warmer months [*Betts et al.*, 1999; *Baldocchi et al.*, 2000]. This second factor is one focus of this paper, which addresses the differences between different sites in the NSA on diurnal and seasonal timescales, and the integrating role of the daytime boundary layer (BL). In addition, we present a discussion of the impact of the net radiation and wind on the near-surface vertical stratification at night. Our last topic is the diurnal and seasonal variation in surface CO_2 fluxes and CO_2 concentration, and their links to the stable nocturnal boundary layer and the seasonal cycle of temperature.

2. Data Sets

We shall use data from five sites: three of which were BOREAS flux tower sites and two that were mesonet sites with meteorological and radiation instrumentation. Table 1 summarizes the sites, their location and elevation, the canopy height, and the principal heights of the measurements used in this paper (the fen and young jack pine sites had instruments at several other levels). The instrumentation at the mesonet sites is summarized by *Shewchuk* [1997], at the fen and young jack pine sites in the work of *Lafleur et al.* [1997], *McCaughey et al.* [1997], *Joiner et al.* [1999a, 1999b] and at the old black spruce site in the work of *Goulden et al.* [1997] and *Betts et al.* [1999]. Note that all the sites are located at a similar latitude and elevation, and they are within about 50 km in longitude. These data and their full documentation are all available on the BOREAS CD-ROM set [*Newcomer et al.*, 2000].

3. Spatial and Temporal Variability

The two mesonet sites at Thompson, Manitoba, and the NSA old jack pine (NOJP) site, about 50 km west of Thompson, collected data with a 15-min averaging period over a 3-year period (1994-1996), which will be used for several analyses. We shall focus first on two aspects of the surface climate: the seasonal cycle and the diurnal cycle. Although canopy heights were similar at these sites, the vegetation and soils were quite different, so the comparison serves to illustrate the spatial variability in the boreal forest.

3.1. Seasonal Cycle of Surface Radiation, Surface Temperature, and Humidity

The seasonal cycles of surface radiation, surface temperature, and humidity are discussed first, because they both control the surface energy and water cycle at high latitudes and are also a response to the surface ecological and thermal controls. Figure 1a shows the 3-year (1994-1996) average annual cycle of incoming short-wave radiation (SWin) and net radiation (R_n) at the surface for the two mesonet sites (Thompson, site 8 and the NOJP site 9). The annual cycle is very large at this latitude, and it drives the very large seasonal cycle of temperature. However, there is also a visible and important asymmetry in Figure 1a. In April, both SWin and R_n are considerably larger than in August. This must be a consequence of lower cloud cover in April, associated with the RH minimum (shown in Figure 1c), since the mean solar zenith angle is greater in April than in August. Net radiation is also impacted by the albedo, but albedo is low at these conifer sites, even in April, when there is snow under the canopy [*Betts and Ball*, 1997]. Figure 1b shows the corresponding average annual cycle of temperature. The solid lines are mean temperature, T (at 18.9 m height for Thompson, site 8 and 18.5 m at NOJP, site 9), about 6 m above the canopy at the base of the atmospheric boundary layer. The differences in temperature at this level are very small on the seasonal scale. The dotted and dashed lines, however, labeled with the site numbers, are ground temperatures (at 10 cm and 50 cm depth, respectively). Here below ground, the intersite differences are very large. The annual cycle of soil temperature at the jack pine site (with a sandy soil, and only a thin lichen ground cover) is much larger than at the mixed spruce site at Thompson, where there is an organic soil with a thick overlying moss layer. At this site the annual cycle of temperature at 50 cm is small, and the soil at this depth is still frozen in June. This subsurface heterogeneity is an important feature of the landscape and, along with the vegetation type itself, affects surface fluxes; since, for example, water is unavailable for transpiration until the snow melts and the ground thaws in spring [*Jarvis and Linder*, 2000]. However, the subsurface heterogeneity of temperature is not seen above the canopy in the seasonal cycle. Figure 1c shows the annual cycle (1994-1996) of relative humidity (RH) above the canopy, showing the remarkable seasonal asymmetry over the boreal forest. In spring (April is month 4) when temperatures are still below freezing but the solar elevation and the net radiation are

Table 1. Sites and Data Levels Used in This Analysis From the BOREAS NSA

Station Name	Long., W	Lat., N	Elevation, m	Vegetation Height, m	Site Type Data levels (m)
Thompson (8)	-97.92	55.80	221	spruce/poplar 13	mesonet 1.8, 18.9
NOJP (9)	-98.64	55.93	282	old jack pine 12.8	mesonet 4.6, 18.5
Nfen	-98.42	55.915	211	fen (sparse)	flux 2.5, 4.5, 7.5
NYJP	-98.29	55.90	249	young jack pine 5.8	flux 1.6, 9, 10.3
NOBS	-98.48	55.88	259	old black spruce 10	flux 27, 29

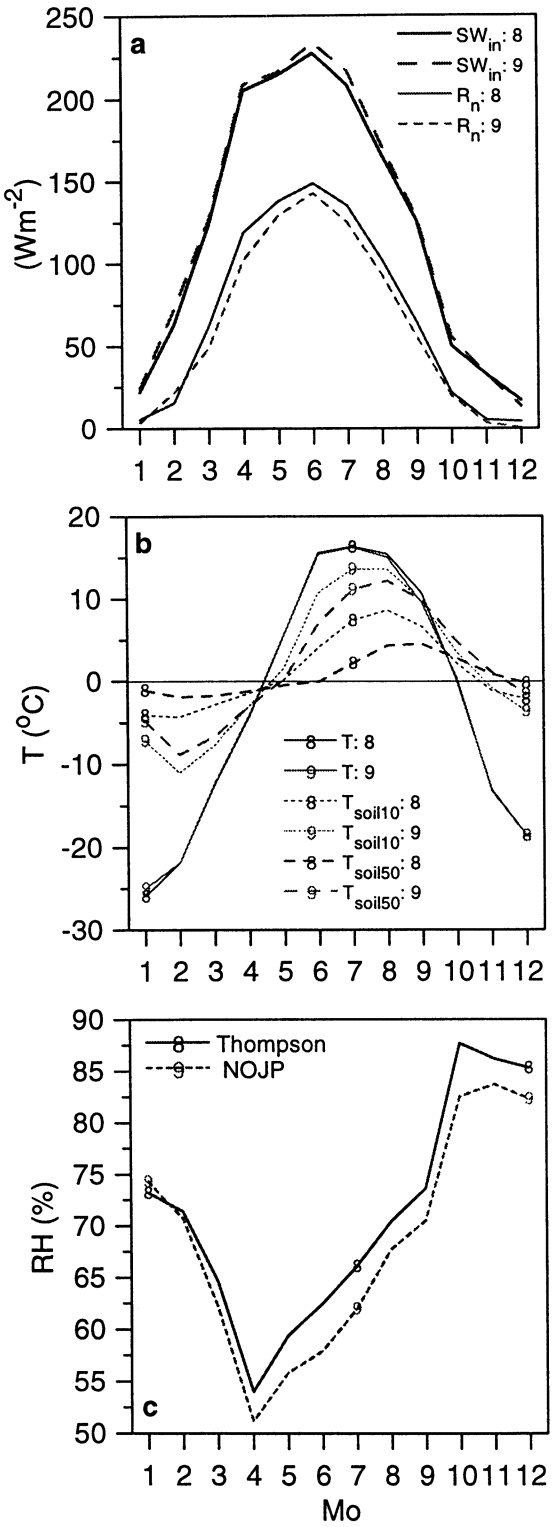

Figure 1. (a) Annual cycle of incoming short-wave radiation and net radiation at two mesonet sites, (b) air temperature and soil temperature, and (c) relative humidity.

increasing rapidly, the RH is a minimum. The minimum daytime RH is very low, often below 25%, because water is generally not available for evaporation at the surface. Evaporation is so low in spring that the forest could be thought of as a "green desert." Consequently, the dry boundary layer in spring can be as much as 2000 m deep, driven by very large sensible heating with very little evaporation [*Betts et al.*, 1996, 1999]. Throughout the spring, summer, and early fall, mean RH rises to an October peak as the surface becomes warm relative to the atmosphere. In October the ground has not frozen at either site, and water is readily available for evaporation. This seasonal asymmetry in RH is in sharp contrast to the seasonal thermal cycle with a midsummer maximum, and is an important characteristic of the northern latitudes. It is linked to the seasonal phase lag of ground temperature, coupled to the phase change of soil water. The jack pine site is slightly drier by 2-3% than the mixed spruce site, probably because there is much less water stored in the sandy soil [*Cuenca et al.*, 1997]. However, the difference between the sites is at the limit of accuracy (nominally ±2%) of the RH sensors (type, Campbell Scientific HMP35CF).

3.2. Diurnal Cycle

Figure 2a shows for the two mesonet sites the diurnal cycle of temperature (an April-July mean for 1994-1996) at four levels: at 10 cm and 50 cm below ground, a lower sensor (T_L) under the canopy, 1.8 m above ground at Thompson, and 4.6 m at NOJP, and the upper sensors (T_+) near 19 m, about 6 m above the canopy. Local noon is near 1830 UTC. Not surprisingly, considering the different annual cycles shown in Figure 1a, below-ground temperatures are warmer and the diurnal cycle is larger at the jack pine site. Indeed at Thompson, there is almost no diurnal cycle below ground, and the 4-month mean temperature at 50 cm depth is just marginally above freezing. Above the canopy (solid lines) the diurnal cycle at Thompson is a little larger than at the jack pine site. The mixed spruce site has a lower albedo of 8% [*Betts and Ball*, 1997] than the jack pine site (12%), and correspondingly a higher net radiation, which probably accounts for the slightly larger daytime temperatures above the canopy at Thompson. However, below the canopy and at night, the temperatures at Thompson are cooler, consistent with the lower ground temperatures.

Figure 2b shows the mean diurnal cycle of mixing ratio for the same 4 months. The sites closely track each other, although the spruce site at Thompson with the moss surface above peat (rather than lichen on sand) is systematically wetter, day and night. The diurnal cycle has two interesting peaks. After sunrise at about 1100 UTC, the surface evaporation is trapped beneath the surface inversion. The morning peak in mixing ratio occurs just before the nocturnal inversion is broken, and the boundary layer (BL) rapidly deepens into the preexisting BL [*Barr and Betts*, 1997], when mixing ratio falls. At sunset the BL shrinks again and the mixing ratio rises just above the canopy. The fall of mixing ratio at night to a minimum at the sunrise temperature minimum is probably caused by the formation of dew or frost on the surface (for which we have no measurements).

Figure 2c shows the diurnal cycle of RH above the canopy for both sites; the mixed spruce site at Thompson is consistently wetter, as in Figure 1b. Note that the differences between the sites are larger at night than during the daytime, when the surface is coupled to the BL. The final Figure 2d in this panel (which closely resembles an inversion of Figure 2c) shows P_{LCL}, the pressure height to the lifting condensation (LCL). The line $P_{LCL} = 0$ represents saturation at the surface. This is the presentation we shall generally show to represent humidity because it is very closely related to BL depth (the height of cloud base) during the daytime. In addition, this drop of saturation at the surface is linked to the availability of water for evaporation (see later and also *Betts and Ball* [1995, 1997] and *Betts* [2000]). RH and P_{LCL} are directly linked through the relationship [*Betts*, 1997]

$$P_{LCL}/p_0 = (1-\mathrm{RH})/(A+(A-1)\mathrm{RH}), \quad (1)$$

where p_0 is surface pressure, and the thermodynamic coefficient $A = (\varepsilon L/2C_pT)$, where $\varepsilon = 0.622$ is the ratio of the gas constants for

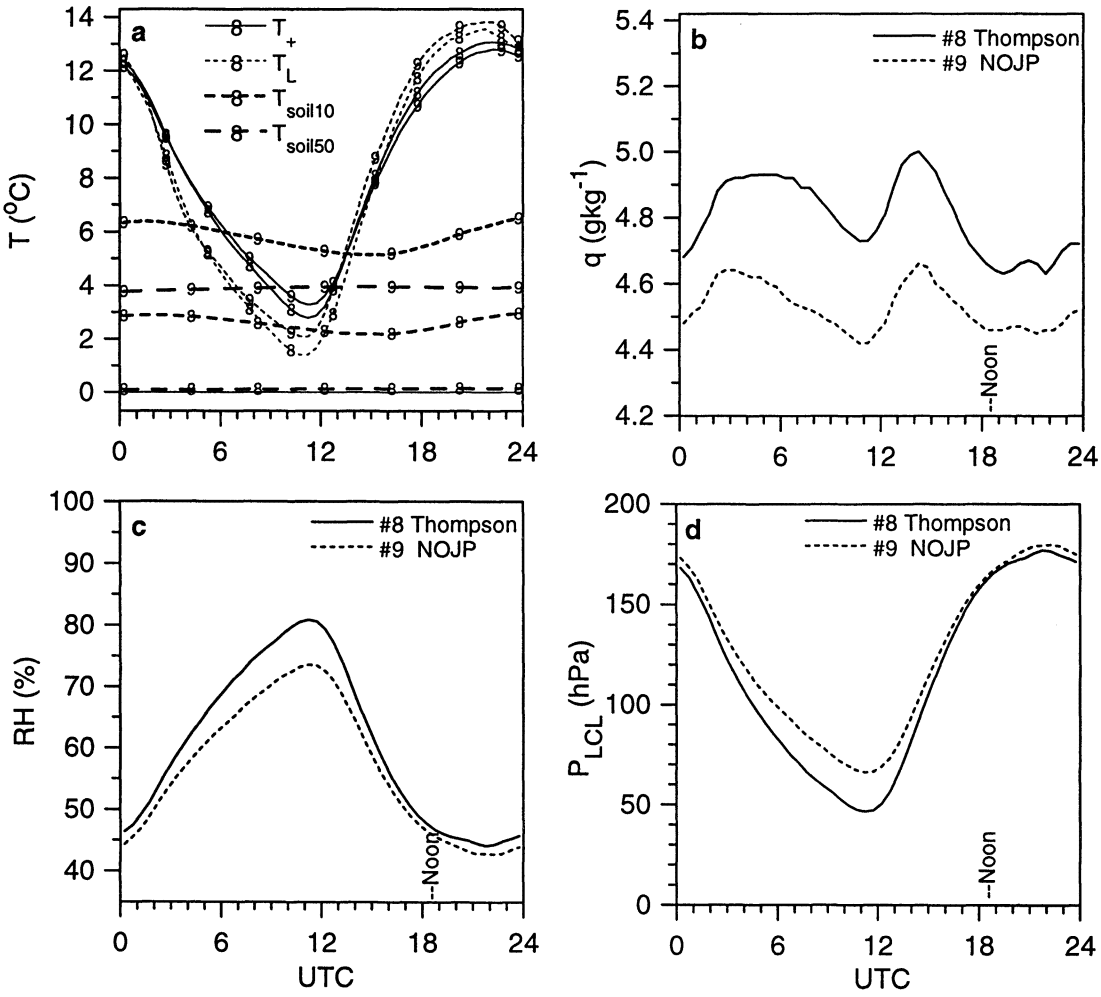

Figure 2. April-July mean diurnal cycle of temperature, mixing ratio, RH, and P_{LCL} for mesonet stations at Thompson and NSA old jack pine.

dry air and water vapor, L is the latent heat of vaporization of water, and C_p is the specific heat of air at constant pressure. The thermodynamic coefficient A increases from 2.6 to 3.4 as temperature decreases from 25°C to -40°C.

3.3. Seasonal Cycle of Diurnal Cycle

This section shows the seasonal cycle of the diurnal cycle of temperature and P_{LCL}. Figure 3a shows the mean diurnal cycle of temperature from April (month 4) to October (month 10) for the Thompson site, a mean for the 3 years 1994-1996. The peak daytime temperatures are barely above freezing in April and rise rapidly to maximum in July and August, before falling again. In October, when the Sun angle is low, the mean diurnal cycle is small and near freezing again.

Figure 3b shows the seasonal trend of P_{LCL} for Thompson. P_{LCL} falls (and RH rises from (1)) almost monotonically from April to October both during the day and at night (consistent with Figure 1b). The particularly sharp fall from September to October is probably not just a local effect but associated in part with the systematic advection of shallow BLs from the north. Figure 3c is the corresponding trend of P_{LCL} for the old jack pine site 50 km to the west. The pattern is very similar, showing that this seasonal trend is not local. At night, Thompson is systematically closer to saturation in all months (consistent with Figure 2d, and the lower mean wind speeds shown later in Figure 8), but in the daytime, the differences between the sites are much smaller (the differences in August and September are due to missing data at NOJP). Figure 4 shows similar graphs of P_{LCL} for the NSA young jack pine site and fen site from June to October (an average, for the 2 years 1994 and 1996, when there are data). The daytime structure is similar at both sites and to Figures 3b and 3c, but at night at the northern fen site (where the measurements are 7.5 m above ground), conditions are similar and close to saturation in all months. The measurements suggest that the daytime structure of the diurnal and seasonal cycles is similar at all four sites. The difference between these two sites at night is illustrated in Figure 5, which shows summer averages (for June to August 1994) for the highest and lowest sensor pairs. The top panel shows P_{LCL} (and RH on the right-hand scale) and the bottom panel shows temperature. The thick solid line is the NYJP site at 10.3 m, above the canopy (the tallest trees are about 5.8 m high), while the thick line is at 1.6 m beneath the canopy. Under the canopy the air becomes uncoupled at night from the atmosphere above, the temperature falls by radiative cooling and convection off the canopy, and the RH rises above 90%. The vegetation at the fen site is low, with only sparse shrubs reaching a few meters in height. At night, the air at both levels cools sharply and decouples from the atmosphere above, very much like the air under the jack pine canopy. During the daytime, mean temperatures at both upper sensors are very close, while it is a little warmer and drier under the

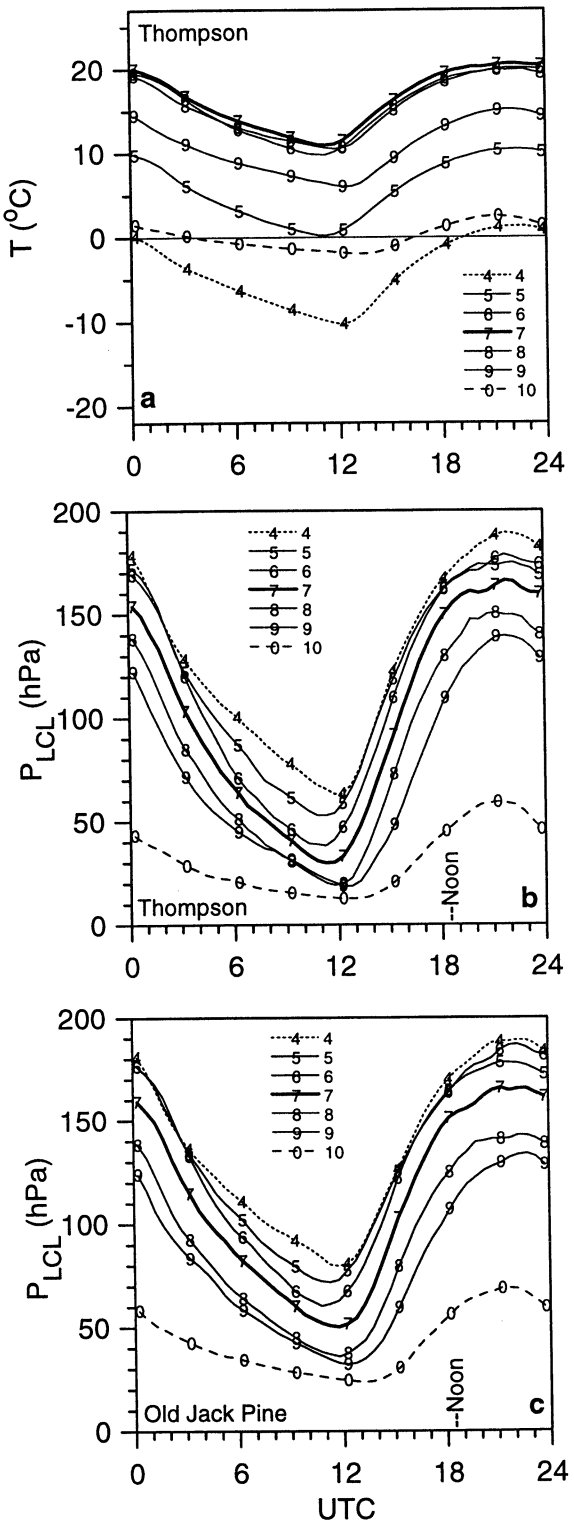

Figure 3. Diurnal cycle of above canopy temperature (top), and P_{LCL} for Thompson (middle), and P_{LCL} for old jack pine site (bottom).

jack pine canopy than at 2.5 m over the fen, consistent with the lower evaporative fraction at the jack pine site (see section 3.5).

3.4. Vertical Gradients of Temperature

The vertical gradients of temperature through the canopy are of interest for two reasons. They indicate the extent of the coupling between canopy and atmosphere and are of interest also because of the link between temperature and respiration. The bottom panel of Figure 5 illustrates the stable BL that is set up through the canopy at night in the warm season at the young jack pine site. During the day the gradient reverses. The strength of the stable stratification at night depends strongly on wind speed. At high wind speeds, turbulence mixes air down through the canopy, and the vertical temperature is small, but at low wind speeds, the stable temperature gradient increases inside the canopy, as the forest becomes decoupled from the atmosphere. *Bosveld et al.* [1999] discuss the physics of this uncoupling process in some detail, and our less extensive measurements are broadly consistent with their conclusions. We will use the 3 years of data from the two mesonet sites in the warm season to show the links between nighttime stability, wind speed, and net radiative cooling.

Figure 6 shows the diurnal cycle of the temperature difference between the temperature sensors below (at above ground heights of 1.8 m and 4.6 m, see Table1) and about 6 m above the canopy,

$$\Delta T = T_L - T, \tag{2}$$

binned as a function of wind speed U above the canopy for May-September 1994-1996. The top panel is for the mixed spruce site at Thompson, and the bottom panel for the old jack pine site. They show the same pattern. At night for wind speeds below 2 m s-1,

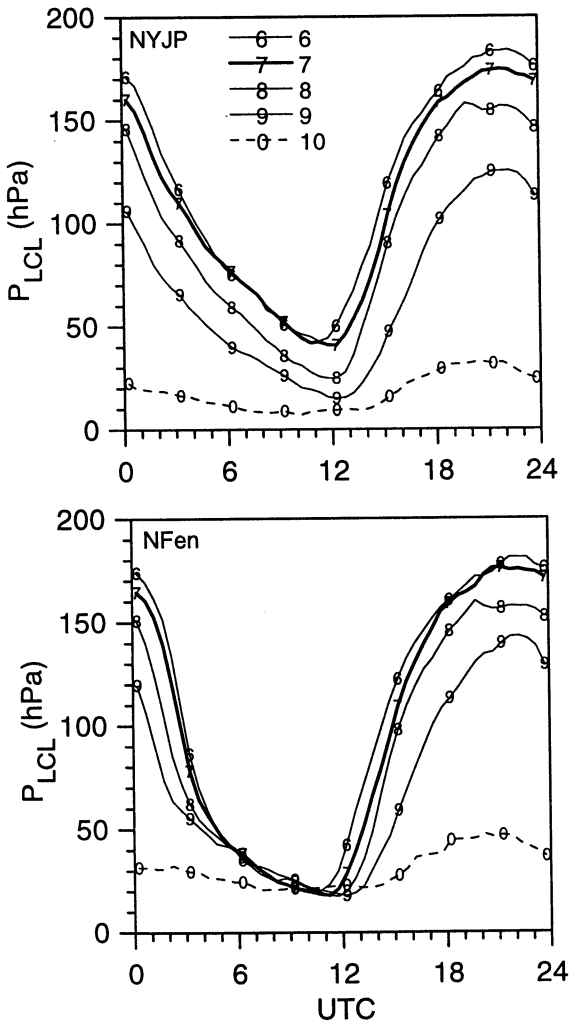

Figure 4. Average diurnal cycle of P_{LCL} for NSA young jack-pine site (top) and fen site (bottom) for summers of 1994 and 1996.

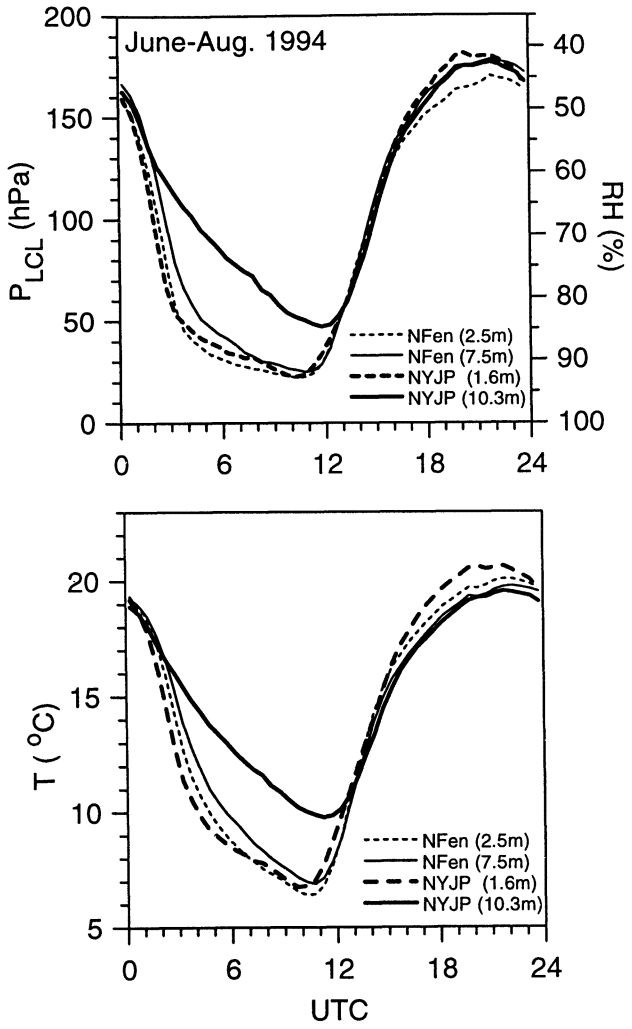

Figure 5. Comparison of P_{LCL} and RH (top) and temperature (bottom) for upper and lower sensors at NFen and NYJP sites, averaged for June, July, and August 1994.

there is a -2 K stable stratification across the canopy, but the stable temperature gradient disappears as wind speeds increase. The threshold for decoupling for these sites appears to be about 3 m s^{-1} for a wind-speed measurement height of 19 m above a 13 m canopy, consistent with the value of 3.5 m s^{-1}, reported by *Bosveld et al.* [1999] for a higher reference height of 36 m above a dense Douglas-fir forest with a mean stand height of 18m. The thick line is the mean for the summer. For the nighttime period 0400-1000 UTC the mean value of ΔT is -1.6 K for both sites.

This decoupling appears to be a function of both the external forcing parameters; the wind speed above the canopy driving the turbulent mixing and the net long-wave cooling, which drives the radiative fall of temperature. Figure 7 bins ΔT for this 0400-1000 UTC period for the same months as a function of wind speed above the canopy and net radiation. The mean stable stratification across the canopy increases as expected with decreasing wind speed and increasing outgoing net radiation. For the slightly more open jack pine site with a sandy soil, ΔT reaches -5 K for wind speeds below 1 m s^{-1} and R_n < -55 W m^{-2}. *Bosveld et al.* [1999] suggested that the critical wind speed for uncoupling could be estimated as

$$U_c = (R_n/5.5)^{0.5}, \quad (3)$$

which is closely consistent with the trend shown in Figure 7, although both measurement and canopy heights here are lower than theirs. The bottom panel shows a simple parameterization of this dependence, using the critical wind speed from (3)

$$\Delta T = (U - U_c)(R_n/30), \quad (4)$$

with ΔT in degrees Kelvin, U_c in meters per second and R_n in Watts per square meter, which is a reasonable mean fit to the data at these two sites. This temperature gradient through the canopy is certainly of ecological significance, and (4) might be a useful simple parameterization for that purpose.

Figure 8 shows the frequency of occurrence (percent) in the ranges of R_n and wind speed for the 0400-1000 UTC nighttime time block (May-September 1994-1996) for the two sites. Wind speeds are slightly higher on average at the old jack pine site (which is at a higher elevation). This explains why the mean curves in Figures 6 and 7 are quite close, although the ΔT is larger at the old jack pine site in a given wind speed and net radiation class. The lower mean wind speeds at Thompson are also probably in part the reason why in Figures 2 and 3 the air above the canopy at Thompson is a little cooler and closer to saturation at night.

3.5. Seasonal Cycle of Surface Fluxes

The previous sections have explored the diurnal, seasonal and vertical thermodynamic structure over the boreal forest. This section shows the monthly mean diurnal cycle from April to October of the

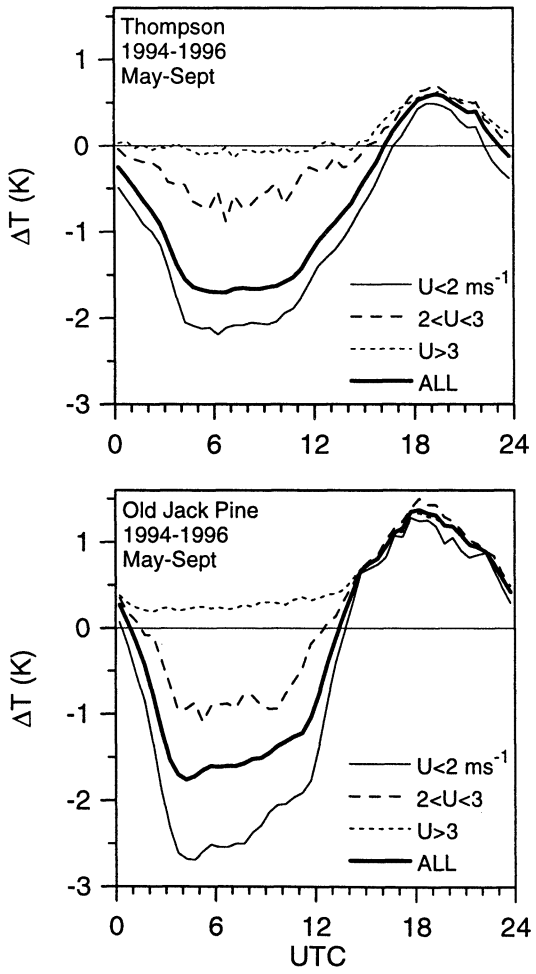

Figure 6. Temperature difference ΔT between below and above canopy as a function of wind speed for Thompson (top) and old jack pine sites (bottom).

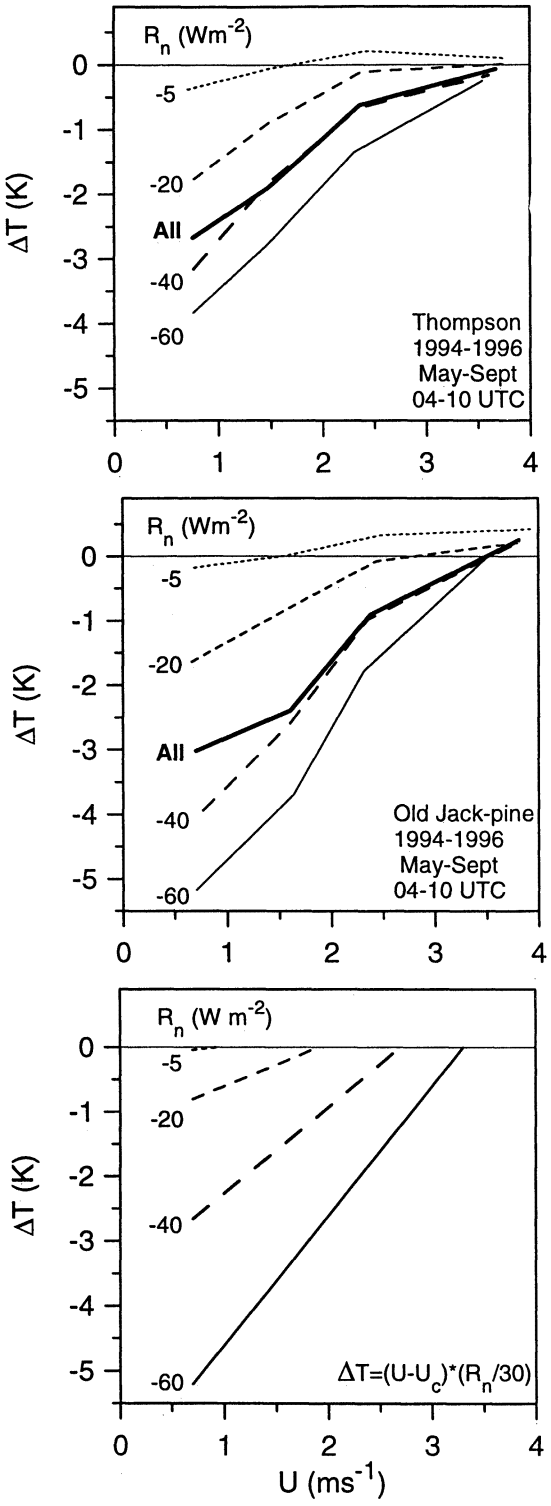

Figure 7. Nighttime (0400-1000 UTC) mean ΔT from below to above canopy, stratified by wind speed and net radiation above canopy for Thompson (top), old jack pine (middle), and model equation (4) (bottom).

surface fluxes. The dominant landscape class in the BOREAS northern study area is wet conifers [*Goulden et al.*, 1997; *Barr et al.*, 1997; *Steyaert et al.*, 1997], represented by the old black spruce site 40 km west of Thompson (Table 1). Figure 9 shows the 1994-1996 monthly mean diurnal cycle of sensible heat (SH) (top panel) and latent heat (LH) (bottom panel). There are some periods of

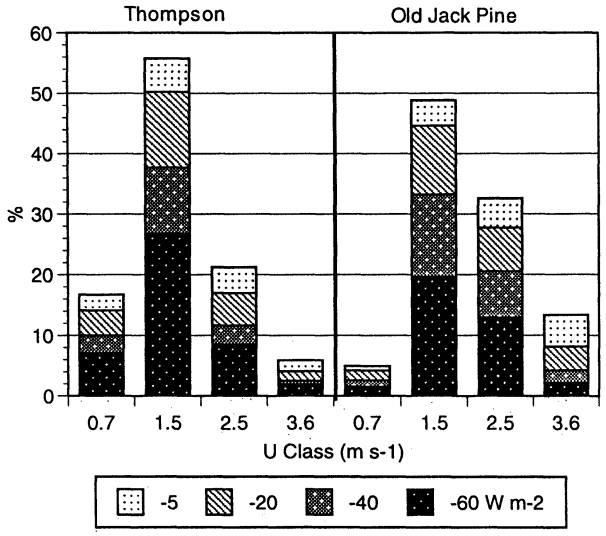

Figure 8. Frequency distribution of classification of nighttime data in Figure 7.

missing data [*Goulden et al.*, 1997; *Betts et al.*, 1999], so we have simply binned all the available data in a given month. The seasonal trend of SH is almost a monotonic decrease from a daytime peak in April (dotted) of 300 W m^{-2} to an October (dashed) daytime

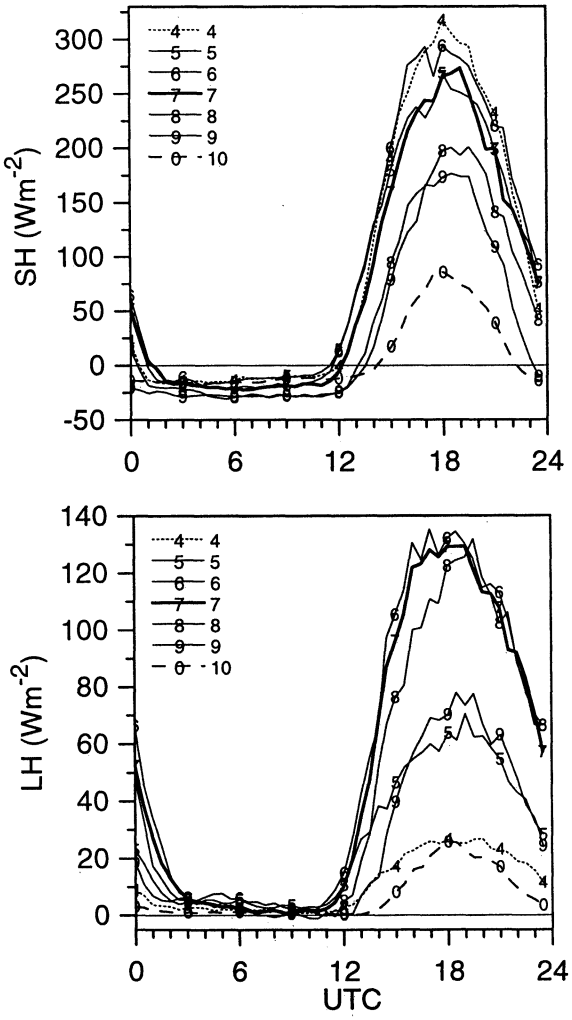

Figure 9. Diurnal cycle of SH and LH from April to October for the NSA old black spruce site.

maximum of barely 80 W m^{-2}. In sharp contrast, LH has a more symmetric seasonal structure. It is similar and low in April and October (peak about 30 W m^{-2}), higher in May and September, and reaches its seasonal maximum with a daytime peak around 130 Wm-2 in June, July, and August.

Figure 10 shows the seasonal cycle of a 10-day average evaporative fraction (EF) and precipitation for the three flux sites. For NOBS the average is for the 3 years 1994-96, while for NFen and NYJP, only 2 years are included, 1994 and 1996. The mean 10-day precipitation is shown for both the three- and the two-year averages. EF was derived by first averaging the SH and LH fluxes in 10-day bins (there are some gaps in the data) and then calculating from the means

$$EF = LH/(LH+SH). \quad (5)$$

The seasonal record is longest at the NOBS site. Before the spring thaw, which occurs around day 140 in middle to late May, EF is very low, less than 0.2, because the ground is frozen and the snow lies under the canopy. There is a quick rise with the thaw that can be seen at both the conifer sites to daily average values around 0.4. followed by a slight rise in EF toward the late summer. At the NYJP site, which is on porous sandy soil, there are larger fluctuations of EF in summer (rainfall is low in all 3 years from days 240-260) than at the NOBS site, which has a wet organic soil overlying clay with a surface moss layer [*Betts et al.*, 1999; *Harden et al.*, 1997]. The fen site, where water is generally freely available for evaporation and the dominant species are deciduous, has quite a different seasonal cycle. EF also rises steeply with the thaw and leaf-out in spring to daily average summer values above 0.6, much higher than at the conifer sites. In late summer and fall, EF falls as the fen dries out. Note that EF at the fen, in sharp contrast to the nearby jack pine site, shows little variation in EF with corresponding 10-day rainfall (shown dashed for the 1994 and 1996 average). In the NSA there was no flux site at a stand of deciduous forest. However, measurements in the southern Study Area show that the seasonal cycle of EF at an aspen site [*Blanken et al.*, 1997; *Barr et al.*, this issue] is similar to that at the NFen site. However, since the NSA landscape is dominated by conifers, these also dominate mean evaporation on the landscape scale. The general rise of EF from spring to fall at the conifer sites is the main cause of the seasonal rise of RH shown in Figure 1b.

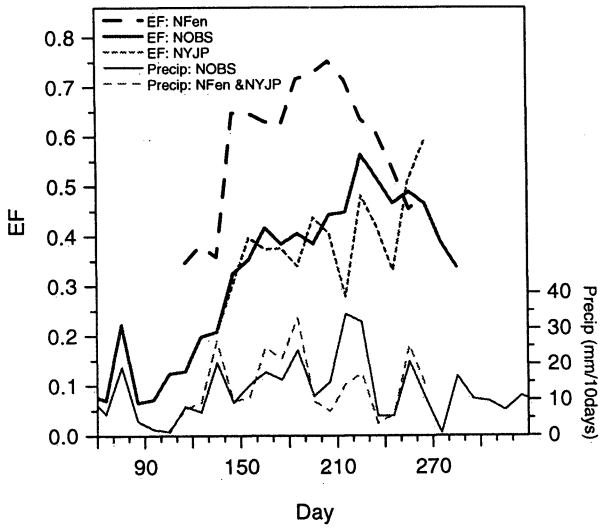

Figure 10. Seasonal cycle of 10-day average evaporative fraction and precipitation for NOBS (1994-1996), NFen, and NYJP (for 1994 and 1996).

3.6. Seasonal Trend of CO_2 and CO_2 Uptake

The links between the diurnal and the seasonal cycle of temperature and the CO_2 uptake are of climatic importance [*Wofsy et al.*, 1993; *Black et al.*, 1996; *Baldocchi et al.*, 1997; *Keyser et al.*, 2000]. We will show here local mean time series and discuss local processes, although part of the signal observed locally comes from larger-scale advective processes. Figure 11 has three panels showing the diurnal cycle of mean CO_2, net CO_2 uptake, and temperature above the canopy for the old black spruce site (NOBS), created by simply binning the 3 years of data from 1994 to 1996. (There are a few data gaps that have not been filled in.) We show the separate months May to October and an average (thick dashes) of the six cold months November to April (which we shall loosely call winter). For this "winter" season (when mean temperatures are well below zero, bottom panel), mean CO_2 (for 1994-1996) is around 366 ppm and has almost no diurnal cycle, because photosynthesis and respiration are negligible [*Winston et al.*, 1997]. Figure 11b shows that there is a small CO_2 loss from the forest with again no diurnal cycle for the corresponding winter period. As the forest warms in May, respiration increases and nighttime mean CO_2 rises, falling again with daytime photosynthesis. As temperature rises, the diurnal cycle of CO_2 increases to a maximum in July, while the amplitude of the diurnal cycle of CO_2 flux peaks a month later in August, before falling again in September and October. The thick solid curves are the 3-year annual mean curves.

Figure 12 compares (on the same scale) the three sites, NOBS, NYJP, and NFen, for the months June to October 1996. By October 1996 (which was the coldest of the three Octobers of 1994-1996 with daytime mean temperatures barely rising above freezing) the diurnal cycle (thick dotted) is flat indicating no biological activity, and within a few parts per million of 365 ppm at each site. Similarly, during the months of June to September the daytime values at the sites have a similar variation and lie within a few parts per million. The sole exception is June at the fen site, which is lower than at the conifer sites, perhaps because of an earlier onset of photosynthesis. At night the rise of CO_2 resulting from respiration into the stable BL is very similar at the two conifer sites, where the measurements are above the canopy (at 29 m for NOBS and 10m for NYJP). However, at the fen site, where the measurement is at 4.5 m (and night time temperatures are much colder as seen in Figure 5, indicating a more stable stratification), the rise of mean CO_2 is more than a 100 ppm in July and August, about 4 times the rise over the conifer sites.

We present Figures 11 and 12 to show the challenge for fully coupled land surface modeling. The features shown represent processes at many scales. The local diurnal cycle of CO_2 is partly a reflection of local photosynthetic uptake and respiration and the diurnal cycle of local BL depth. However, we have as yet no long-term measurements of CO_2 above the surface to analyze the BL CO_2 budget. Although the daytime BL effectively homogenizes the atmosphere, particularly above the canopy on scales of the order of 100 km, near-surface conditions under the nocturnal BL are more heterogeneous and are linked to the vertical stability. Moreover, the black spruce site, where we have near-continuous measurements over many years is only a small part of the landscape. This site has very little net uptake in the years 1994-1996 [*Goulden et al.*, 1997]. Figure 11 also shows the fall of CO_2 to a minimum in August. This involves not just local uptake but the summer uptake in the Northern Hemisphere as a whole. Since again we have no continuous measurements of the CO_2 above the local BL (in the air which is advected from greater distances), we cannot separate local and large-scale processes. Nonetheless, as our global models move toward Earth system models with a fully coupled carbon cycle, the CO_2 diurnal cycles shown in Figures 11 and 12 are a good local

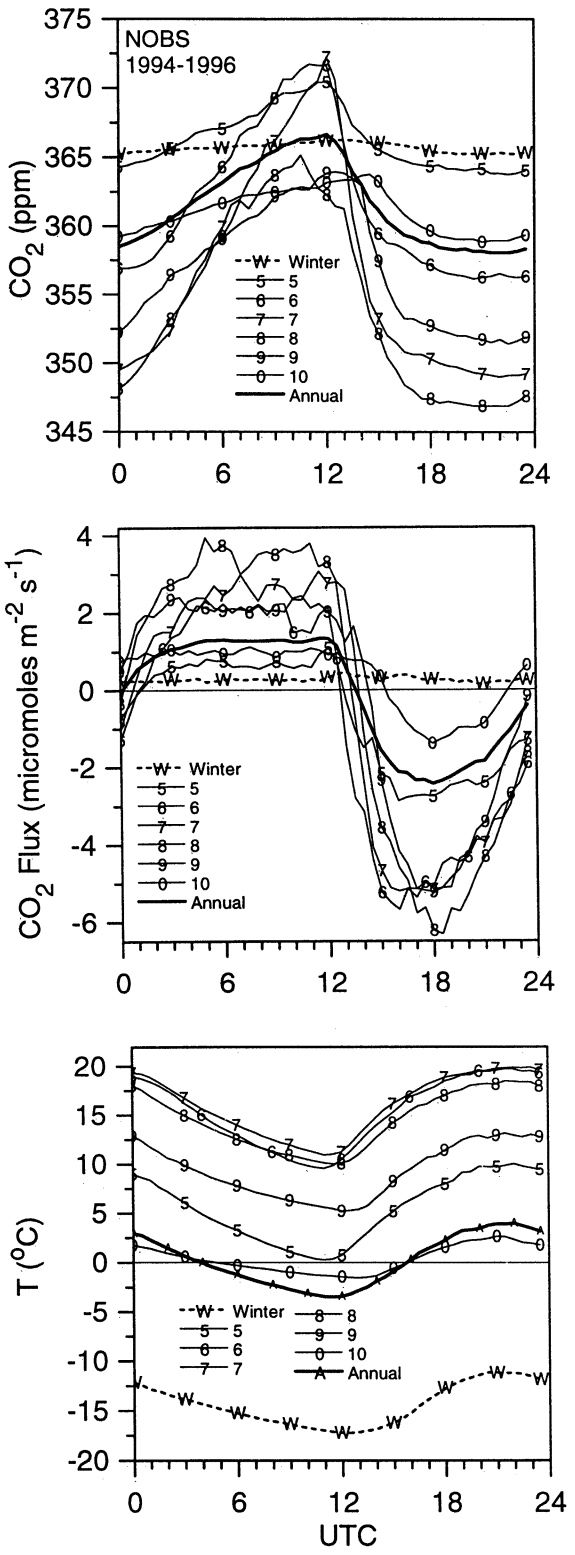

Figure 11. Diurnal cycle of mean CO_2, net CO_2 flux, and above-canopy temperature for old black spruce site.

measure of the fully coupled system. Like the thermodynamic variables, the CO_2 concentration shows that conditions are much more homogeneous between sites in the daytime, when the surface is well coupled to an unstable nearly well-mixed BL than under the heterogeneous stable BL at night.

4. Some Important Physical Processes at the Surface in the Boreal Forest

We have already discussed in section 3 some of the links between many physical processes over the boreal forest. Some, such as understanding the full CO_2 budget over the forest, need further data and analysis. Our analysis of the vertical stratification at night is also restricted largely to the warm season and to two sites. In this section we will comment further on just three processes that are important for the boreal forest climate.

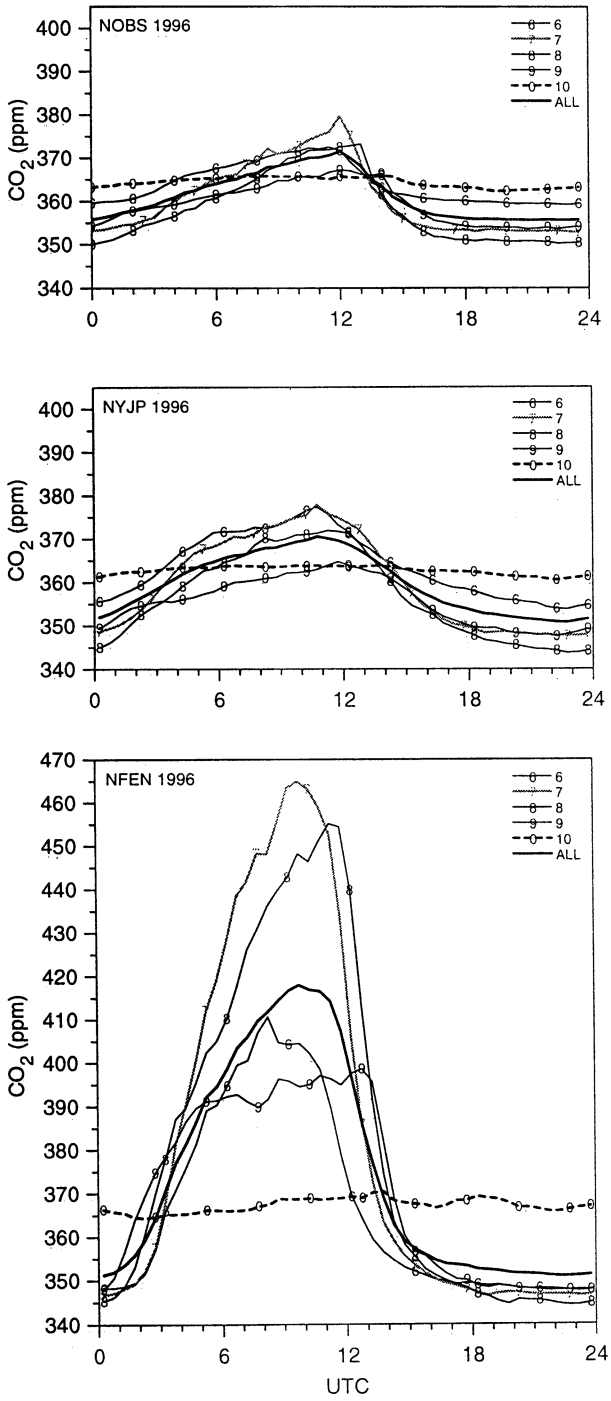

Figure 12. Comparison of monthly mean diurnal cycle of CO_2 for three sites in 1996.

4.1. Role of Albedo and Freeze-Thaw Processes for Forests, Wetlands and Lakes

The northern forests and wetlands are regions of sharply contrasting albedo, so this plays an important role in the surface energy balance on both short timescales and the annual timescale. *Betts and Ball* [1997] showed that in summer the conifer sites have a very low albedo <0.1, comparable to the albedo of the lakes, while deciduous and grass sites have a significantly larger albedo (0.15-0.2). In winter the contrast is very large between forest, where the snow is beneath the canopy and shaded from the low sun angles, and albedo only rarely exceeds 0.2, and the open sites and frozen lakes, which can have albedos in the range 0.6-0.8 [*Joiner et al.*, 1999b; *Rouse*, 2000] depending on the age of the snow. In global models, errors in the mean albedo of the forest, wetland, and lake system can have a large impact on surface temperature forecasts before snowmelt in spring [*Viterbo and Betts*, 1999]. The length of the snow-free or unfrozen period has a marked impact on the annual net radiation balance of open areas and lakes at high latitudes (the "snow-albedo feedback" of climate models) but not for the forested areas, where the annual range of albedo is smaller. The presence of the low-albedo forest may maintain a higher mean annual temperature than in a region at the same latitude without forest, even though snow melts earlier at open sites. Recent off-line calculations by *Betts, R. A.* [2000] suggests that the forcing represented by the albedo difference between forests and low vegetation might offset the carbon sequestration by the boreal forests in the planetary energy budget.

The freezing and thawing of the soil also plays an important role in the climate at high latitudes. Winter temperatures are moderated by two processes. The first is the role of the snowpack as an insulator of the soil. The second is the freeze process, which increases the effective heat capacity of the soil by a factor of 20 [*Viterbo et al.*, 1999]. This freeze-thaw introduces a significant lag into the climate system. In spring a significant part of the net radiation goes into melting the snowpack, thawing the ground [*Rouse*, 2000], and melting the lakes (and in warming them). This energy becomes available in fall and the early winter, when the surface refreezes. Water is not available for transpiration in spring until the snow melts and the ground thaws, and for evaporation until the ground, wetlands and lakes warm with respect to the atmosphere. *Jarvis and Linder* [2000] suggest that it is the snowmelt that first introduces liquid water into the soil profile. As discussed above, this unavailability of liquid water leads to very low EF in spring, with large sensible heat fluxes off the forest canopy, which in turn produce deep dry boundary layers in spring [*Betts et al.*, 1996]. In fall, when the lakes and ground are warm relative to the cooling atmosphere, the situation reverses. Evaporative fraction is high for the conifers and lakes (but not for the deciduous species after leaf fall). Net radiation is much lower by the time the surface freezes, so sensible heat fluxes are very low and boundary layers in fall become very shallow, often capped by stratocumulus.These

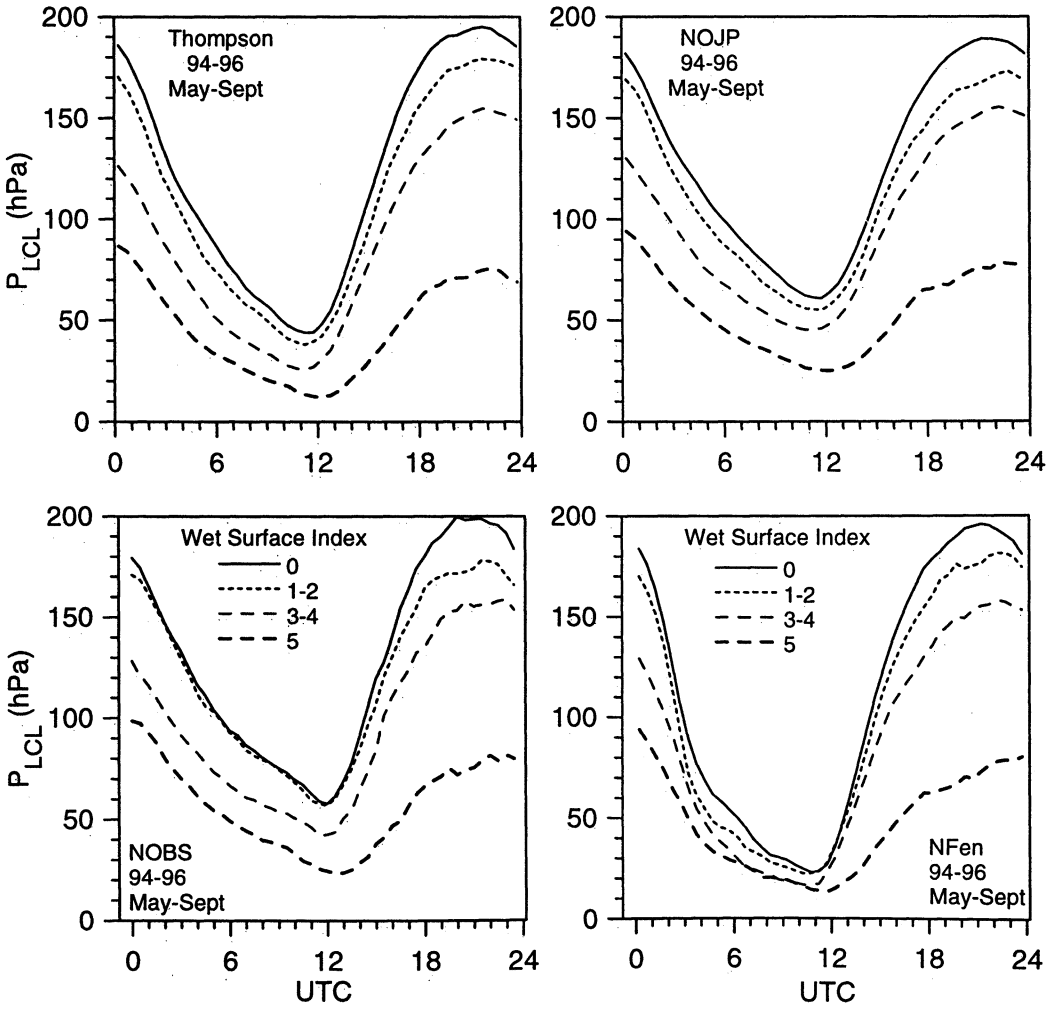

Figure 13. Diurnal cycle of P_{LCL} for four sites, stratified by wet surface index.

seasonal changes in BL are shown as graphs of P_{LCL} in Figure 3. In spring the ground thaw, which occurs when daytime temperatures rise well above freezing, is the key control on surface evaporation. Two of the important surface controls on summer transpiration in the boreal forest will now be addressed.

4.2. Coupling to Surface Water Availability

Betts et al. [1999] showed that one important control on evaporation from the NSA old black spruce site was the amount of water stored on the surface and in the surface moss layer. They assigned a wet surface index (WS) to each day based on the rainfall on preceding days. We assigned this wet surface index for the NSA to all five surface sites in Table 1 and stratified P_{LCL} by WS for the months of May to September 1994-1996 as shown in Figure 13 for four of the sites: Thompson, the old jack pine site, the old black spruce site, and the fen (which has very little data for 1995). The four panels are very similar, showing that P_{LCL}, which is a measure of BL depth (and RH), is quite homogeneous over the NSA during the daytime. The more stable nighttime BL at the fen has been discussed earlier in conjunction with Figure 5. The daytime surface fluxes, however, show wide differences from site to site. Figure 14 shows the same stratification by WS of EF for the black spruce site (top panel) and the NFen (middle panel), and NYJP site (bottom). EF varies with WS for the black spruce site as the water stored in the moss layer directly affects evaporation [*Price et al.*, 1997; *Betts et al.*, 1999]. This is not true for the fen since, not surprisingly, water is generally available regardless of recent rainfall. The bottom panel is the young jack pine site. *Joiner et al.* [1999a] show that at the NYJP site EF fell as a function of volumetric soil water from 0.5 after rainfall events to below 0.25 after a week without rain. This is consistent with our graph, where EF increases with WS. However, for this site there is no moss water storage, and the reason is the timescale of storage in the sandy soil, which is also several days [*Cuenca et al.*,1997; *Joiner et al.*, 1999a].

Our conclusion is that while the processes at the surface are heterogeneous, the daytime atmospheric BL is nearly homogeneous on the 50 km scale and dominated by water availability at the conifer sites. Specifically, recent rainfall has a large influence on evaporation and BL depth.

4.3. Importance of Stomatal Control by Conifers

The well-known importance of the stomatal control of transpiration by a coniferous forest [e.g., *Jarvis and McNaughton*, 1986) was confirmed by BOREAS [*Jarvis et al.*, 1997; *McCaughey et al.*, 1997; *Goulden et al.*, 1997; *Betts et al.*, 1999]. The diurnal cycles of EF at the three flux sites in Figure 14 have important differences, even though there is little difference in the atmospheric forcing. At the northern fen, EF climbs from midmorning to midafternoon as evaporation increases with falling RH (see top panel of Figure 5, for example). At the black spruce site, EF does not rise as RH falls to its afternoon minimum, indicating that stomatal control is playing a role. At this site, part of the evaporation is from the moss layer [*Price et al.*, 1997; *Betts et al.*, 1999] and EF has a broad daytime minimum. At the jack pine site, where water is most limited because of the sandy soil, the solid curve in the bottom panel of Figure 14, for the driest soil conditions, shows that EF drops to a minimum in midafternoon about the time of the RH minimum. Here stomatal control, enhanced by the low soil moisture, must be the strongest. Figure 15 illustrates this important climatic role more clearly. We compare the link between measured evaporation from the NYJP and NFen sites, RH and net radiation, by averaging the daytime data (1200-2400 UTC) from the months June to October 1994 and 1996 into 10% bins in RH and 100 Wm^{-2} bins of net radiation. During the daytime the atmospheric

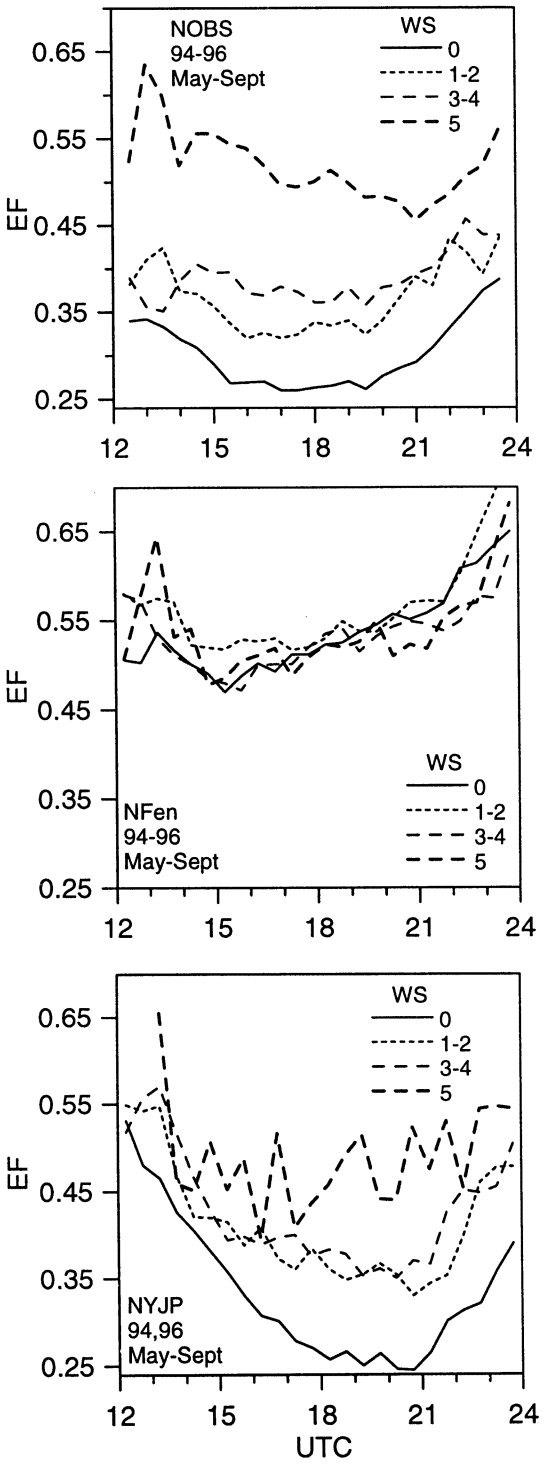

Figure 14. Daytime diurnal cycle of evaporative fraction for NOBS, NFen, and NYJP, stratified by wet surface index.

forcing variables of temperature and humidity differ little between the sites, as discussed previously, but evaporation has a totally different behavior. Evaporation increases with R_n as expected for both sites. At the fen, evaporation increases with decreasing relative humidity, consistent with the high availability of water. However, at the jack pine site, where soil moisture is generally low due to the sandy soil, at low radiation levels, evaporation is flat with decreasing RH, and at high radiation levels, evaporation actually falls as RH decreases. Thus we see that at low RH the evaporation

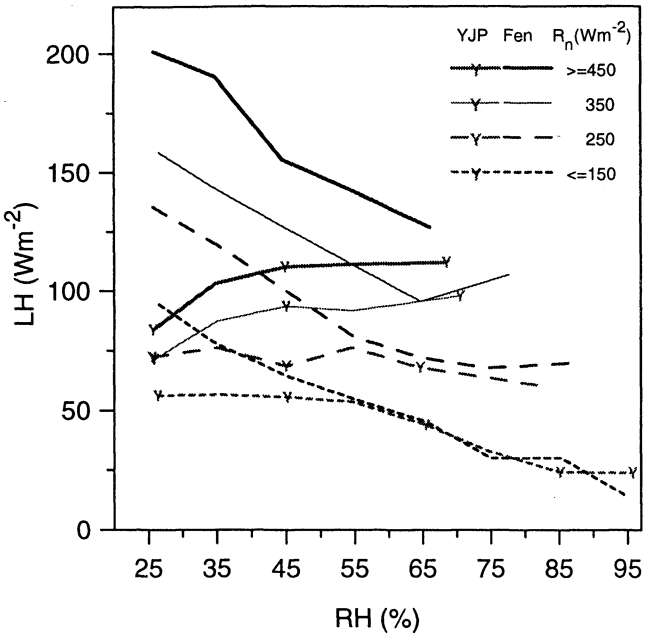

Figure 15. Distinct dependence of surface evaporation on relative humidity and net radiation for NFen and NYJP sites.

curves diverge widely, even though the atmospheric drivers are almost identical. Since the landscape is dominated by a coniferous forest with strong stomatal control, the climatic equilibrium of the diurnal cycle is controlled by the forest, not the fens. In addition, because evaporation is low despite high R_n, near-surface RH is low and the diurnal cycle of P_{LCL} is large; while at the same time, the fens are not in equilibrium with the overlying dry BL and have a much higher surface evaporation. We show the dependence of LH on RH rather than vapor pressure deficit (VPD), which has been widely used in the study of canopy physiology, because VPD has a strong temperature dependence, and the important atmospheric variables RH and P_{LCL} are tightly linked through (1). In addition, *Betts et al.* [1999] found that vegetative resistance, inferred from data at the NSA old black spruce site was more tightly correlated with T and RH than T and VPD. The link among equilibrium evaporation, equilibrium BL depth, and vegetative resistance is discussed more extensively by *Betts* [2000].

5. Conclusions

This paper summarizes some of the important processes that affect near-surface climate over the boreal forest, using data from the BOREAS northern study area just west of Thompson, Manitoba. The boreal forest is marked by a very large seasonal cycle with below freezing temperatures for half the year. Snow cover and the freezing and thawing of the soil plays an important role in the climate at high latitudes. Both moderate winter temperature, because snow insulates, and during the freeze process the effective heat capacity of the soil is greatly increased, which introduces a significant lag into the system. In spring, a significant part of the net radiation goes into melting the snow, thawing the ground, and melting the lakes (and in warming them). This energy becomes available in fall and early winter, when the surface again freezes. One important consequence is that water is unavailable for evaporation and photosynthesis until snowmelt and ground thaw, which occurs late in spring. In April and early May, although the boreal forest is "green", RH is a minimum, the surface SH flux is large, and daytime BLs are very deep, because of this unavailability of water. In addition, because of lower cloud cover, the incoming solar radiation and surface net radiation is significantly higher in April than in August, despite the slightly lower solar elevation. We came to think of the boreal forest as a "green desert" in spring. The situation reverses in the fall, when the ground is warmer than the cooling atmosphere, and mean RH is high and BL depths low. This asymmetry between spring and fall in humidity can be seen in both seasonal and diurnal cycles.

The forest is heterogeneous, and there is a marked difference in summer in daytime evaporative fraction between the conifers and the deciduous forest and fens. However, above the forest the daytime BL has a strong homogenizing effect, and it is the dominant coniferous forest that controls the mean BL depth. The impact of recent rainfall, stored on the canopy, in the surface moss layer, and in the top soil layer can also be readily seen in summer. In composites, mean BL depths rise on succeeding days without rain. A comparison of the fen and young jack pine sites shows the important role of the stomatal control by conifers on transpiration. Since evaporation goes down at high net radiation and low RH for conifer sites, it is clear that the generally low RH and high BL depth over the forest are a direct consequence of stomatal control. At night, however, temperature, relative humidity, and CO_2 are quite heterogeneous under the stable BL. The stable BL is strongest at the fen site, and consequently at nighttime in summer, the air is closest to saturation and has the highest CO_2 values. The uncoupling of the stable BL inside the forest canopy occurs at low wind speeds and high outgoing net radiation at night and can lead to as much as a 5K cooling within the canopy, which may be of importance to physiological processes such as respiration.

Acknowledgments. Alan Betts was supported by NASA under grants NAG5-7377 and NAG5-8364 and the National Science Foundation under grant ATM99-88618. The efforts of the many BOREAS scientists who collected and analyzed these data are greatly appreciated, and we are particularly grateful to Steve Wofsy and Michael Goulden for the northern black spruce data.

References

Baldocchi, D.D., C. Vogel, and B. Hall, Seasonal variation of carbon dioxide exchange rates above and below a boreal jack pine forest, *Agric. For. Meteorol., 83*, 147-170, 1997.

Baldocchi, D.D., F.M. Kelliher, T.A. Black and P. Jarvis, Climate and vegetation controls on boreal zone energy exchange, *Global Change Biol., 6*, 69-83, 2000.

Barr, A.G., and A.K. Betts, Radiosonde boundary layer budgets above a boreal forest, *J. Geophys. Res, 102*, 29,205-29,212, 1997.

Barr, A.G. A.K. Betts, R. Desjardins, and J. I. MacPherson, Comparison of regional surface fluxes from boundary-layer budgets and aircraft measurements above boreal forest, *J. Geophys. Res, 102*, 29,213-29,218, 1997.

Barr, A. G., A K. Betts, T.A. Black, J.H. McCaughey, and C.D. Smith, Intercomparison of BOREAS northern and southern study area surface fluxes in 1994, *J. Geophys. Res.*, this issue.

Betts, A.K., The parameterization of deep convection, chap. 10, in *The Physics and Parameterization of Moist Atmospheric Convection*, NATO ASI Ser. C, Edited by R. K. Smith, vol. 505, pp. 255-279, Kluwer Acad., 1997.

Betts, A. K., Idealized model for equilibrium boundary layer over land, *J. Hydrometeorol., 1*, 507-523, 2000.

Betts, A.K., and J.H. Ball, The FIFE surface diurnal cycle climate,. *J. Geophys. Res., 100*, 25,679-25,693, 1995.

Betts, A.K., and J. H. Ball, Albedo over the boreal forest, *J. Geophys. Res.*, 102, 28,901-28,913, 1997.

Betts, A. K., and J. H. Ball, FIFE surface climate and site-average dataset:1987-1989, *J. Atmos. Sci., 55*, 1091-1108, 1998.

Betts, A. K., and P. Viterbo, Hydrological budgets and surface energy balance of seven subbasins of the Mackenzie River from the ECMWF model, *J. Hydrometeorol., 1*, 47-60, 2000.

Betts, A. K., J.H. Ball, A.C.M., Beljaars, M.J. Miller, and P. Viterbo, The

land-surface-atmosphere interaction: A review based on observational and global modeling perspectives, *J. Geophys. Res.*, *101*, 7209-7225, 1996.

Betts, A.K., P. Viterbo, A.C.M. Beljaars, H.-L. Pan, S.-Y. Hong, M. L.Goulden, and S.C. Wofsy, Evaluation of the land-surface interaction in the ECMWF and NCEP/NCAR reanalyses over grassland (FIFE) and boreal forest (BOREAS), *J. Geophys. Res.*, *103*, 23,079-23,085, 1998.

Betts, A. K., M. L. Goulden, and S.C. Wofsy, Controls on evaporation in a boreal spruce forest, *J. Clim.*, *12*, 1601-1618, 1999.

Betts, A. K., P. Viterbo, A.C.M. Beljaars, and B.J.J. M. Van den Hurk, Impact of BOREAS on the ECMWF forecast model, *J. Geophys. Res.*, this issue.

Betts, R. A., Offset of the potential carbon sink from boreal forestation by decreases in surface albedo, *Nature*, *408*, 187-190, 2000.

Black, T.A., et al., Annual cycle of water vapor and carbon dioxide above a boreal aspen forest, *Global Change Biol.*, *2*, 219-229, 1996.

Blanken, P.D., T.A. Black, P.C. Yang, H.H. Neumann, Z. Nesic, R. Staebler, G. den Hartog, M.D. Novak, and X. Lee, Energy balance and canopy conductance of a boreal aspen forest: Partitioning overstory and understory components, *J. Geophys. Res.*, *102*, 28,915-28,927, 1997.

Bosveld, F. C., A.A.M. Holtslag, and B.J.J.M. Van den Hurk, Nighttime convection in the interior of a dense Douglas-fir forest, *Boundary Layer Meteorol.*, *93*, 171-195, 1999.

Cuenca, R. H., D.E. Stangel, and S.F. Kelly, Soil water balance in a boreal forest, *J. Geophys. Res.*, *102*, 29,355-29,365 1997.

Goulden, M.L., B.C. Daube, S.-M. Fan, D.J. Sutton, A. Bazzaz, J.W. Munger, and S.C. Wofsy, Physiological Responses of a Black Spruce Forest to Weather, *J. Geophys. Res.*, *102*, 28,987-28,996,1997.

Harden, J.W., K.P. O'Neill, S.E. Trumbore, H. Veldhuis, and B.F. Stocks, Moss and soil contributions to the annual net carbon flux of a maturing boreal forest, *J. Geophys. Res.*, *102*, 28,805-28,816, 1997.

Jarvis, P. G., and S. Linder, Constraints to growth of boreal forests, *Nature*, *405*, 904-905, 2000.

Jarvis, P. G., and K. G. McNaughton, Stomatal control of transpiration, *Adv. Ecol. Res.*, *15*, 1-49, 1986.

Jarvis, P. G., J. M. Massheder, S. E. Hale, J. B. Moncrieff, M. Rayment and S. L. Scott, Seasonal variation of carbon dioxide, water vapor, and energy exchanges of a boreal black spruce forest, *J. Geophys. Res.*, *102*, 28,953-28,966, 1997.

Joiner, D. W., J. H. McCaughey, P. M. Lafleur, and P.A. Bartlett, Water and carbon dioxide exchange at a boreal Young Jack Pine site in the BOREAS northern study area, *J. Geophys. Res.*, *104*, 27,641-27,652, 1999a.

Joiner, D. W., P. M. Lafleur, J. H. McCaughey and P.A. Bartlett, Interannual variability in carbon dioxide exchanges at a boreal wetland in the BOREAS northern study area, *J. Geophys. Res.*, *104*, 27,663-27,672, 1999b.

Keyser, A.R., J.S. Kimbal, R.R. Nemani and S.W. Running, Simulating the effects of climate change on the carbon balance of North American high-latitude forests, *Global Change Biol.*, *6*, 185-195, 2000.

Lafleur, P. M., J. H. McCaughey, D.W. Joiner, P.A. Bartlett, and D.E. Jelinski, Seasonal trends in energy, water and carbon dioxide fluxes at a northern boreal wetland, *J. Geophys. Res.*, *102*, 29,009-29,020, 1997.

McCaughey, J.H., P.M. Lafleur, D.W. Joiner, P.A. Bartlett, A.M. Costello, D.E. Jelinsky, amd M.G. Ryan, Magnitudes and seasonal patterns of energy, water and carbon exchanges at a boreal young jack pine site in the BOREAS northern study area, *J. Geophys. Res.*, *102*, 28,997-29,008, 1997.

Newcomer J., et al. (Eds.), Collected Data of The Boreal Ecosystem-Atmosphere Study, CD-ROM. NASA, 2000.

Price, A. G., K. Dunham, T. Carleton, and L. Band, Variability of water fluxes through the black spruce (Picea mariana) canopy and feather moss (Pleurozium schreberi) carpet in the boreal forest of northern Manitoba, *J. Hydrol.*, *196*, 310-323, 1997.

Rouse, W. R., The energy and water balance of high latitude wetlands, *Global Change Biol.*, *6*, 59-68, 2000.

Shewchuk, S.R., The surface mesonet for BOREAS, *J. Geophys. Res.*, *102*, 29,077-29,082.

Steyaert, L.T., F.G. Hall, and T.R. Loveland, Land-cover mapping, fire regeneration and scaling studies in the Canadian boreal forest with 1km AVHRR and Landsat TM data, *J. Geophys. Res.*, *102*, 29,581-29,598, 1997.

Van den Hurk, B.J.J.M., P. Viterbo, A.C.M. Beljaars, and A. K. Betts, Off-line validation of the ERA40 surface scheme, *ECMWF Tech. Memo. 295*, Eur. Cent. For Medium-Range Weather Forecasts, Reading, England, 2000.

Viterbo, P., and A.K. Betts, The impact on ECMWF forecasts of changes to the albedo of the boreal forests in the presence of snow, *J. Geophys. Res.*, *104*, 27,803-27,810, 1999.

Viterbo, P., A.C.M. Beljaars, J.F. Mahfouf, and J. Teixeira, The representation of soil moisture freezing and its impact on the stable boundary layer, *Q. J. R. Meteorol.* Soc., *125*, 2401-2426, 1999.

Winston, G.C., E.T. Sundquist, B.B. Stephens, and S.E. Trumbore, Winter CO_2 fluxes in a boreal forest. *J. Geophys. Res.*, *102*, 28,795-28,804, 1997.

Wofsy, S.C., M.L. Goulden, J.W. Munger, S.-M. Fan, P. S. Bakwin, B.C. Daube, S.L. Bassow, and F.A. Bazzaz, Net exchange of CO_2 in a mid-latitude forest, *Science*, *260*, 1314-1317, 1993.

J. H. Ball and A. K. Betts, Atmospheric Research, 58 Hendee Lane, Pittsford, VT 05763 USA. (akbetts@aol.com)

J. H. McCaughey, Department of Geography, Queen's University, Kingston, ON, Canada.

(Received July 31, 2000; revised January 2, 2001;
accepted January 19, 2001.)